

Deep Transfer Learning for Land Use Land Cover Classification: A Comparative Study

Raoof Naushad ^a, Tarunpreet Kaur ^b

^aAccubits Invent – Artificial Intelligence R&D Lab, Accubits Technologies Inc, Trivandrum, India, 695581

^bDepartment of Biomedical Science, Acharya Narendra Dev College, University of Delhi, India, 110019.

Abstract. Efficiently implementing remote sensing image classification with high spatial resolution imagery can provide great significant value in land-use land-cover classification (LULC). The developments in remote sensing and deep learning technologies have facilitated the extraction of spatiotemporal information for LULC classification. Moreover, the diverse disciplines of science, including remote sensing, have utilised tremendous improvements in image classification by CNNs with Transfer Learning. In this study, instead of training CNNs from scratch, we make use of transfer learning to fine-tune pre-trained networks a) VGG16 and b) Wide Residual Networks (WRNs), by replacing the final layer with additional layers, for LULC classification with EuroSAT dataset. Further, the performance and computational time were compared and optimized with techniques like early stopping, gradient clipping, adaptive learning rates and data augmentation. With the proposed approaches we were able to address the limited-data problem and achieved very good accuracy. Comprehensive comparisons over the EuroSAT RGB version benchmark have successfully established that our method outperforms the previous best-stated results, with a significant improvement over the accuracy from 98.57% to 99.17%.

Keywords: Land Use Classification, Land Cover Classification, Remote Sensing, Satellite Imagery, EuroSAT, Earth Observation, Deep Learning, Transfer Learning, Satellite Image Classification

1 Introduction

There have been rapid advancements in remote sensing technologies, satellite image acquisitions, production of unprecedented sources of information and increased access to data availability, allowing us to understand the features of earth more comprehensively, encouraging innovation and entrepreneurship. The enhanced ability to observe the earth from low orbit and geostationary satellites [1] and better spatial resolution for remote sensing data [2] has led to the development of novel approaches for remote sensing image analysis and understanding, thus facilitating extensive ground surface studies.

Scene classification that is aimed at labelling an image according to a set of semantic categories [3] is eminent in the remote sensing field due to its extensive applications including LULC [4,5] and land resource management [2].

The recent years have witnessed great advances in LULC classification in tasks like denoising, cloud shadow masking, segmentation, classification etc. Extensive algorithms have been devised with a concrete theoretical basis, exploiting the spectral and spatial properties of pixels. However, with the increase in the level of abstraction from pixels to objects to scenes, and complex spatial distributions of diverse land-cover types, classification continues to be a challenging task [6]. Object or pixel-based [7 - 9] approaches possessing low-level features encoding spectral, textural and geometric properties become incompetent to capture the semantics of the scene.

Hu et al [10] deduce that more representative and high-level features, which are the abstractions of low-level features are necessary for scene classification. Currently, CNNs are the dominant methods in image classification, detection and segmentation tasks because of their ability to extract high-level feature representations to describe scene images [11].

Hu et al. [10] observed that in spite of CNNs' fine capability to extract the high-level and low-level features, it is tedious to train the CNNs with smaller datasets. Whereas, Yin et al [12] and Yosinski et al. [13] observed that the features learned by the layers from different datasets show common behaviour. Convolution operators from the initial layers learn the general characteristics and towards the final layers, there is a transition to features more specific to the dataset on which the model is trained. These general and specific CNN layer feature transitions lead to the development of transfer learning (TL) [13-15]. As a result, the features learnt by the CNN model

on a primary job are employed for an unrelated secondary task in transfer learning. The primary model acts as a starting point or as a feature extractor for the secondary model.

We aim at making the following contributions in this paper.

- Perform LULC classification using two TL architectures - VGG16 and Wide Resnet-50 on the RGB version of the EuroSAT dataset.
- Empirically evaluate the performance of the methods with and without data augmentation.
- Improve the model performance and computation cost with model enhancement techniques.
- Benchmarking the RGB version of the EuroSAT dataset.

2. Related Work

This section presents the previous studies in remote sensing scene classification using DL and TL. Also, we present state-of-the-art image classification methods for LULC on the EuroSAT dataset.

Jian et al. used Principal Component Analysis (PCA) to reduce data redundancy, then trained a self-organizing network [16] to classify Landsat Satellite images which outperformed the maximum likelihood method. Later, Yushi et al. showed the potential of DL on hyperspectral data classification with a hybrid framework which includes DL, logistic regression and PCA [17]. Stacked autoencoders were used in DL frameworks to extract high-level features. Basu et al. and Zuo et al. used deep belief networks [4, 11] for remote sensing image classification and

experimentally demonstrated the effectiveness of the model. [18, 19] demonstrated the potential of CNNs for LULC classification, where the latter actively selected training examples in each iteration with DL and performed better. The scarcity of labelled data was tackled by implementing data augmentation techniques [20]. Furthermore, [21] improved the generalisation capability and performance by combining deep CNN and multi-scale feature fusion against the limited data. Another constraint with remote sensing images was the presence of scenic variability which limited the classification performance. As a work-around, Saliency Dual Attention Residual Network has been studied in [22] containing both spatial and channel attention, leading to better performance. Later [23] came up with an enhanced classification method involving the Recurrent Neural Network along with Random Forest for LULC. Another approach with an attention mechanism was studied by Alichiri et al. based on the pre-trained EfficientNet-B3 CNN [24]. They have tested it on six popular LULC datasets and demonstrated the capability in remote sensing scene classification tasks. In 2015, Marco et al. did experiments on distinct remote sensing datasets with two architectures - Caffenet and GoogleNet [25]. Instead of training from scratch, they used pre-trained weights and fine-tuned with the datasets. This resulted in a significant improvement in design time, overfitting and improved accuracy. [26, 27] also proposed specific fine-tuning strategies which were better than CNN for aerial image classification. Bahri et al. experimented with a TL technique that outperformed all the existing baseline models by using Neural Architecture Search Network Mobile (NASNet Mobile) [28] as a feature descriptor and also introduced a loss function that contributed to the performance.

Authors	Model	Bands	Accuracy
Chen 2018	Knowledge Distillation	RGB	94.74%
Chong 2020	4-convolution max-pooling layer	All 13 spectral bands	94.90%
Chong 2020	VGG_16	RGB	94.50%
Sonune 2020	VGG_19	RGB	97.66%
Sonune 2020	ResNet-50	RGB	94.25%
Sonune 2020	Random Forest	RGB	61.46%
Helber 2019	GoogleNet	RGB	98.18%
Helber 2019	ResNet-50	CI	98.57%
Helber 2019	ResNet-50	SWIR	98.30%
Helber 2019	ResNet-50	SWIR	97.05%
Li 2020	DDRL-AM	RGB	98.74%
Yassine 2021	CNN	All 13 spectral bands	98.78%
Yassine 2021	CNN	All 13 spectral bands + VIRE + NNIR + BR	99.58%

Table 1: Comparative analysis of studies for LULC classification with EuroSAT dataset

In the context of LULC classification (Table 1) on the EuroSAT dataset, [29] the creators used GoogleNet and ResNet-50 architectures with different band combinations and achieved the best accuracy of 98.57%. Also, the Knowledge Distillation method [30] was used and an accuracy of 94.74% was achieved. Chong et al. achieved an accuracy of 94.5% and 94.9% by using RGB bands and all 13 spectral bands respectively. In [31] Sonune et al. used RGB bands in three approaches - 1) Random Forest with an accuracy of 61.64%, 2) VGG_19 with an accuracy of 97.66% and 3) ResNet_50 model with 94.25% accuracy. Another approach proposed by [32], the DDRL-AM method, obtained an accuracy of 98.74%. Finally, Yassine et al. tried out two approaches [33] for improving the accuracy of EuroSAT dataset. In the first approach, the 13 spectral bands of Sentinel-2 were used for feature extraction, producing 98.78% accuracy. In the second approach, 13 spectral feature bands of Sentinel-2 along with the calculated indices (Blue Ratio, Normalised Near-Infrared etc.) were used for feature extraction, resulting in an accuracy of 99.58%.

3. Methodology

3.1 Project Description

In this paper, we are using TL to carry out LULC classification. In past experiments, several architectures have been proposed and tested for scene classification [17-20]. After experimenting and comparing different pre-trained architectures [21-23], we employed VGG16 and Wide Resnet-50 for the particular use-case. The models are fine-tuned on the RGB version of the EuroSAT dataset and trained using the PyTorch framework, in the Python language. NVIDIA TESLA P100 GPUs available with Kaggle were used for model training and testing.

3.2 Dataset

EuroSAT is a novel dataset, based on the multispectral image data provided by the Sentinel-2 satellite. It has 13 spectral bands consisting of 27,000 labelled and georeferenced images (2,000 - 3,000 images per class) categorised into 10 different scene classes. The image patches contain 64x64 pixels with a spatial resolution of 10m. Fig. 1 demonstrates some sample images from the EuroSAT dataset. The classes covered by the dataset are - Forest, Annual Crop, Highway, Herbaceous Vegetation, Pasture, Residential, River, Industrial, Permanent Crop and Sea Lake.



Fig. 1. EuroSAT dataset sample images. The available classes are Forest, Annual Crop, Highway, Herbaceous Vegetation, Pasture, Residential, River, Industrial, Permanent Crop and Sea Lake.

For the current study, the RGB version of the EuroSAT dataset is being used for training. The labelled EuroSAT dataset is made publicly available at <https://github.com/phelber/eurosat>. The dataset is split into 75/25 ratios for training (20250 images) and validation (6750 images) respectively. Mini-batches of 64 images were used for training purposes.

3.3 VGG16

VGG16, very deep convolutional networks (upto 19 weight layers) demonstrated that the representation depth is beneficial for the classification accuracy [34]. The pre-trained VGG model is trained on the ImageNet dataset having 1000 classes, with the convolutional block possessing multiple convolutional layers. The top layers learn low-level features and the bottom layers learn high-level features of the images. VGG16 pre-trained models expect input images normalised in mini-batches of 3-channel RGB images of shape (3xHxW), where H and W are expected to be 224.

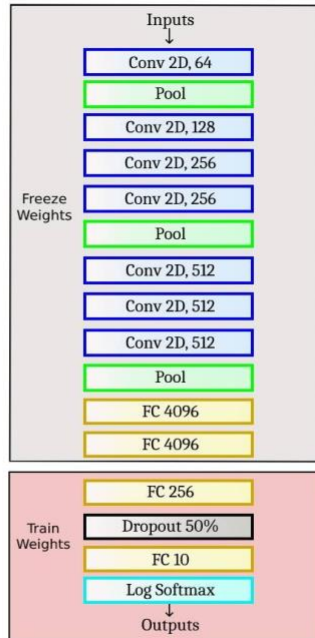
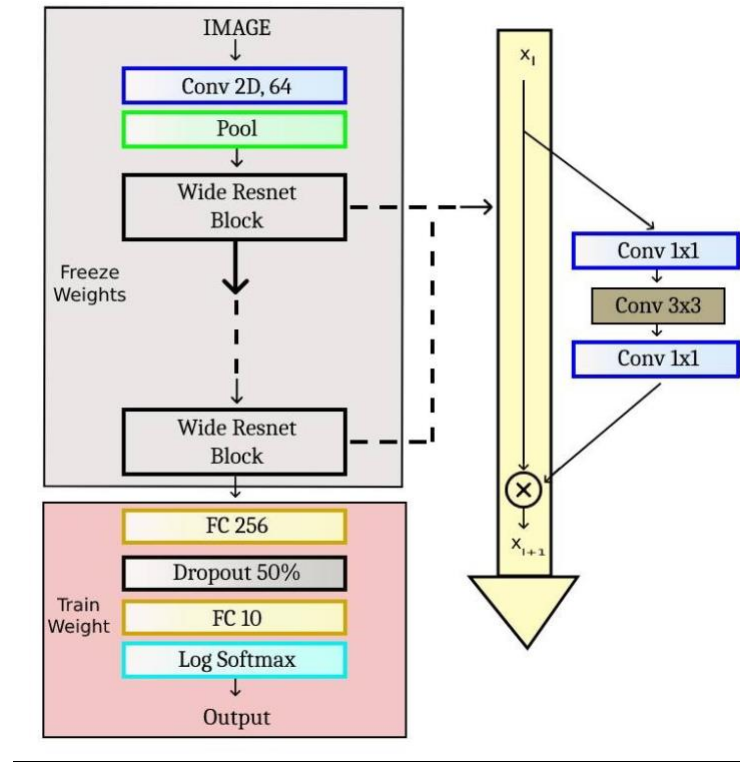


Fig 2. Modified VGG16 architecture with training and freezing layers

3.4 Wide Residual Network

Resnet (Residual Learning framework) can be viewed as an ensemble of many smaller networks and has commendable performance for image recognition tasks [35-37]. The performance degradation problem [38] caused by adding more layers to sufficiently deep networks was tackled by ResNet by introducing - ‘identity shortcut connection’ [39]. The Wide Residual Networks are an improvement over the Residual Networks. They possess more channels with increased width and decreased depth when compared to the Residual Network [40]. WRNs pre-trained models expect input images normalised in mini-batches of 3-channel RGB images of shape (3xHxW), where H and W are expected to be 224.



In the study, we used pre-trained models of Wide Resnet-50 and VGG16. Final classification layers were replaced with fully connected and dropout layers (Fig. 2, Fig. 3). ReLU and log-

softmax activation functions were also used. The initial layers from training were frozen and the modified layer was fine-tuned with EuroSAT dataset. The model was trained for 25 epochs with a batch size of 64. Adam was used as the model optimizer with categorical cross-entropy loss for loss calculation. To enhance the model's efficiency in terms of computation time and performance, model enhancement techniques like gradient clipping, early stopping, data augmentation and adaptive learning rates were used.

4. Model Performance Enhancement Techniques

4.1 Data Augmentation

The diversity and volume of training data play an eminent role in training a robust DL model.

Basic data augmentation [41] techniques enhance the diversity of the data to some extent by introducing visual variability, which helps the model to interpret the information with more accuracy [42]. For the EuroSAT dataset, the data augmentation techniques that are used in this study are Gaussian Blurring, Horizontal Flip, Vertical Flip, Rotation and Resizing. There are many data augmentation techniques available but due to the inherent uniformity in the EuroSAT dataset, most of the data augmentation techniques were not having a significant impact.

4.2 Gradient Clipping

Gradient clipping [43] can prevent vanishing and exploding gradient issues that mess up the parameters during training. In order to match the norm, a predefined gradient threshold is defined. Gradient norms that surpass the threshold are reduced to match the norm. The norm is calculated over all the gradients collectively and the maximum norm is 0.1.

4.3 Early Stopping

Early stopping is a regularisation technique for deep neural networks which stops the training after an arbitrary number of epochs once the model performance stops improving on a held-out validation dataset. In essence, throughout training, we save and update the best model weights, and when parameter changes no longer provide an improvement (after a certain number of iterations), we terminate training and utilise the last best parameters (Fig 4). It reduces overfitting and enhances the generalisation capability of deep neural networks.

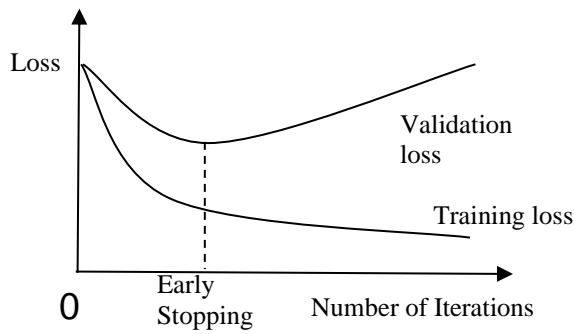


Fig. 4: Early Stopping. Training is stopped as soon as the performance on the validation loss stop decreasing even though the training loss decreases.

4.4 Learning rate optimisation

The learning rate is a hyperparameter that controls how much the model weights are updated in response to the anticipated error in each iteration. Choosing the learning rate may be difficult since a value too small can lead to a lengthy training procedure with significant training error, while a value too big can lead to learning a sub-optimal set of weights too quickly (without reaching the local minima) or an unstable training process [44].

ReduceLROnPlateau [45], Reduce learning rate is used in this investigation. When learning becomes static, models frequently benefit from reducing the learning rate by a factor of 2-10. The

learning rate is lowered by a factor of 0.1 with patience (number of epochs with no improvement) as '2'. We have used Adam as our optimizer maximum learning rate as '1e-4'.

5. Results

We discuss results separately for the two different transfer learning approaches employed for the study. For training each model, all the hyperparameters have been finalised by preliminary experiments. The models have been trained with a 75/25 split for training and testing respectively. We have implemented data augmentation to increase the effective training set size.

5.1 VGG16 (*Very Deep Neural Network*)

We fine-tuned the EuroSAT dataset on VGG16 architecture by freezing the top layers and training only the added classification layers (Fig. 2) with different hyperparameters. The pre-trained weights gave the advantage of the learnings that they have achieved on the ImageNet dataset.

While training without data augmentation (WDA) we were able to achieve a validation accuracy of 98.14% whereas training with data augmentation resulted in better accuracy of 98.55% (Table 2). We have used the early stopping method with patience of 5 and saved the best model with maximum validation accuracy. This approach helped in preventing the overfitting of the model and saved computational time. Due to early stopping, the training stopped at the 21st epoch (18th - WDA) where the total number of epochs was 25. It took 2h 4min 12s for training 21 epochs which means approximately 6.1 minutes for each epoch. But without data augmentation, it took 1h 47min 24s for training 18 epochs, which means approximately 5.9 minutes for each epoch (Table 2).

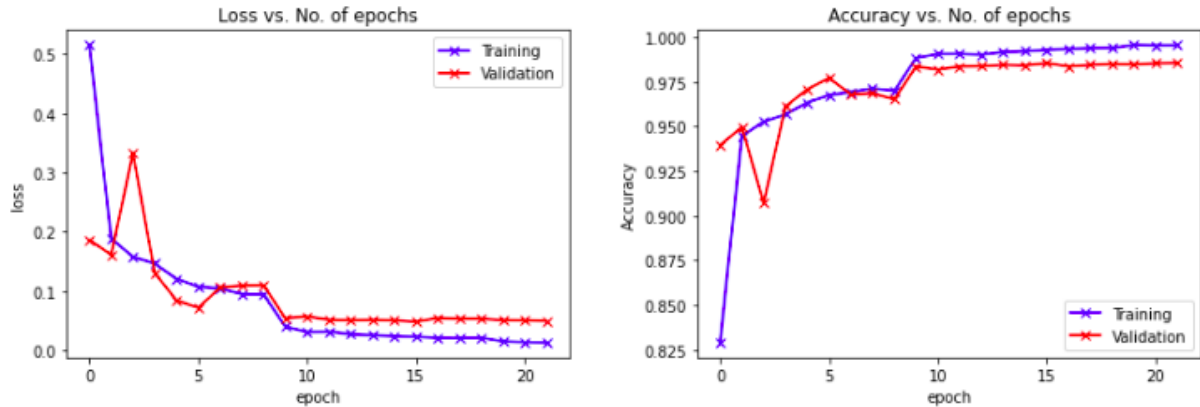


Fig 5. VGG16 results. a) represents the history of training and validation loss across epochs b) represents the history of training and validation accuracy across epochs

Fig. 5, shows the training and validation loss and accuracy diagrams. It demonstrates that from the first epoch itself, both the loss and accuracy have improved exponentially and then shown a linear relation from the 2-10 epochs. During this period, some instability in learning was observed and towards the end, no significant improvement was noticed. Since we have used an adaptive learning rate with ReduceLROnPlateau, the learning rate has updated thrice during the training, which certainly helped the model to achieve the optimum result.

Confusion Matrix for Resnet Approach										
	AnnualCrop	Forest	HerbaceousVegetation	Highway	Industrial	Pasture	PermanentCrop	Residential	River	SeaLake
AnnualCrop	98.41	0	0	0.16	0	1.02	0.81	0	0	0.14
Forest	0	99.73	0	0	0	0.41	0	0	0	0
HerbaceousVegetation	0.26	0	97.39	0	0	1.42	1.79	0	0	0
Highway	0	0	0	98.75	0.49	0	0.16	0	0.64	0
Industrial	0	0	0	0	99.19	0	0	0.52	0.16	0
Pasture	0.66	0	0.78	0	0	97.15	0.16	0	0.16	0.14
PermanentCrop	1.59	0	157	0	0	0.2	95.77	0	0.16	0
Residential	0	0	0	0	0.32	0	0	99.74	0	0
River	0	0	0	0.62	0	0.2	0	0	99.04	0.14
SeaLake	0.13	0	0	0	0	0	0	0	0.32	99.59

Fig 6. Confusion matrix of VGG16

Fig. 6 demonstrates the confusion matrix of VGG16, based on validation data, which shows the class-wise performance of the model. River, Residential, Forest, Sea Lake and Industrial classes show the maximum performance above 99% accuracy whereas permanent crop, herbaceous vegetation and pasture seem to have the least accuracy. Annual crop, Permanent crop, pasture and herbaceous vegetation are getting misclassified because of the similarity in topological features. By analysing the images of these classes it is understood that they share common features that might confuse the model to classify correctly. Fig. 7 shows random sample predictions from the test dataset using the VGG16 model.

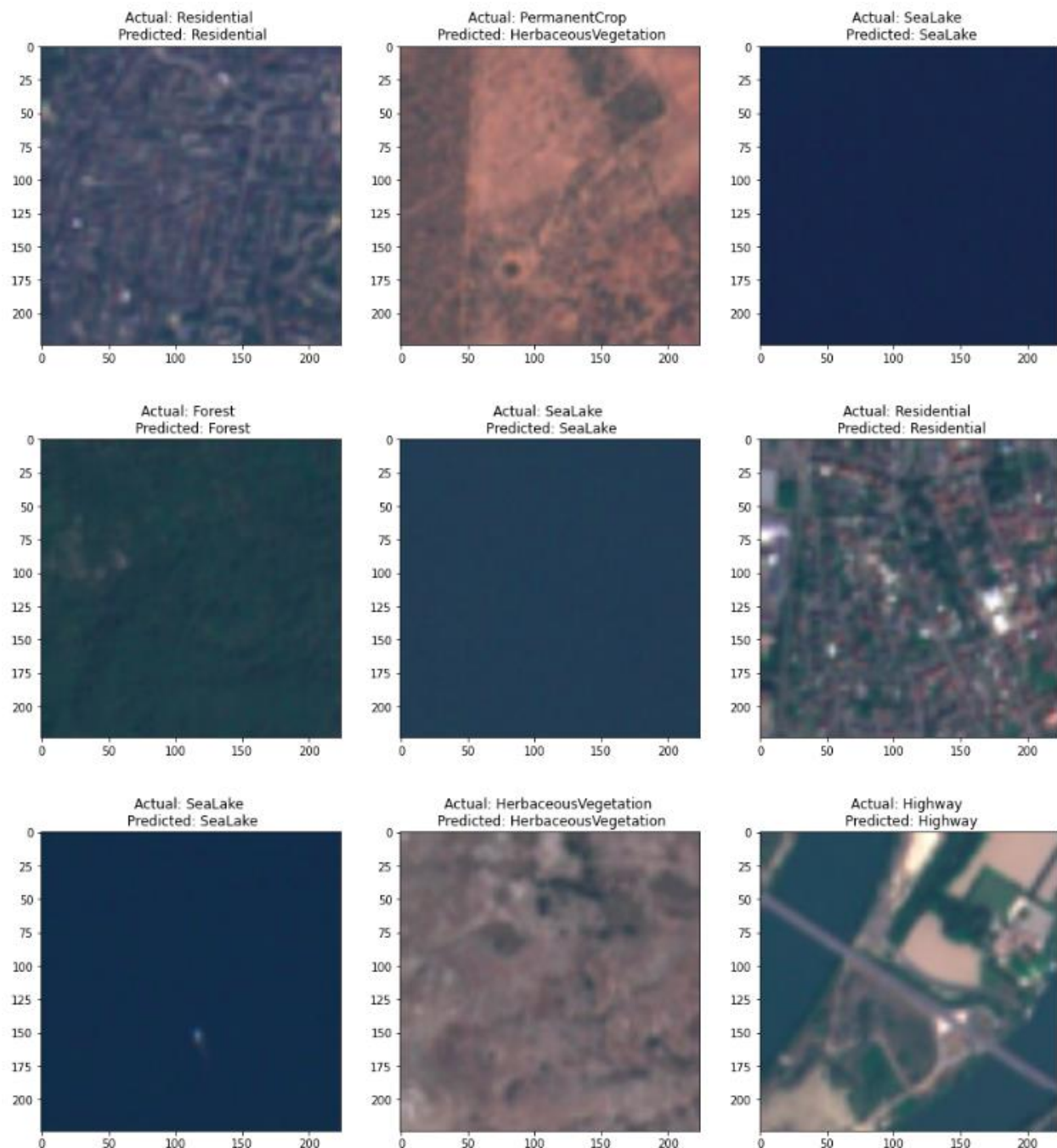


Fig. 7. VGG16 Sample Results. It shows the actual and predicted values of sample inputs from test dataset.

5.2 Wide Resnet-50 (Wide Residual Network)

In the first approach of training WDA, the model was able to achieve a validation accuracy of 99.04% which was outperformed by the approach with data augmentation with an accuracy of 99.17% (Table 2). Hence, the model with the best performance was considered. With early stopping, the training stopped at the 23rd epoch (total 25 epochs) whereas WDA training stopped at the 14th epoch. The best model took 2h 7min 53s to run 23 epochs with 5.6min per epoch, which was better than the VGG16 (Table 2).

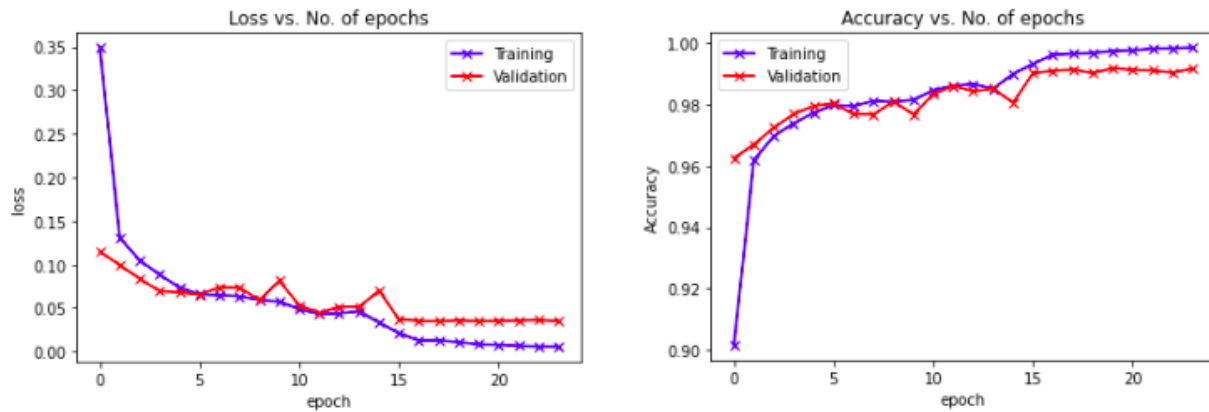


Fig 8. Wide Resnet 50 results. a) represents the history of training and validation loss across each epoch. b) represents the history of training and validation accuracy across each epoch.

Accuracy and loss graphs showed steady learning in the first epoch (Fig. 8). Furthermore, towards the 15th epoch, the learning shows almost a linear relationship. Between the 15th to the 23rd epoch, a delayed and small learning has been achieved because of the updation of the learning rate to smaller optimum values to calculate the best result. The learning rate has changed thrice in the entire training period.

Confusion Matrix for Resnet Approach										
	AnnualCrop	Forest	HerbaceousVegetation	Highway	Industrial	Pasture	PermanentCrop	Residential	River	SeaLake
AnnualCrop	98.81	0	0	0.16	0	0.81	0.49	0	0.16	0
Forest	0	100	0	0	0	0	0	0	0	0
HerbaceousVegetation	0.13	0.27	98.95	0	0	0.41	0.49	0	0	0
Highway	0	0	0	99.22	0.16	0	0	0	0.64	0
Industrial	0	0	0	0.16	99.35	0	0	0.26	0.16	0
Pasture	0.26	0	0.52	0	0	98.78	0	0	0	0
PermanentCrop	0.66	0	0.78	0	0.16	0.2	97.88	0	0	0
Residential	0	0	0	0	0.49	0	0	99.61	0	0
River	0.13	0	0	0.62	0	0	0	0	98.88	0.27
SeaLake	0	0	0	0	0	0	0	0	0.16	99.86

Fig 9. Class-wise confusion matrix of Wide Resnet 50

Fig. 9 shows the confusion matrix for WRN. The forest class is 100% accurate. The classes permanent crop, pasture, annual crop, and herbaceous vegetation are getting misclassified the most, with the least accuracy but with reduced misclassifications as compared to the previous approach. River and Highway classes are also misclassified. When the sample prediction outputs for Wide Resnet-50 and VGG16 were compared using the same inputs, Fig. 10 demonstrates that predictions made using Wide Resnet-50 showed better accuracy than VGG16.

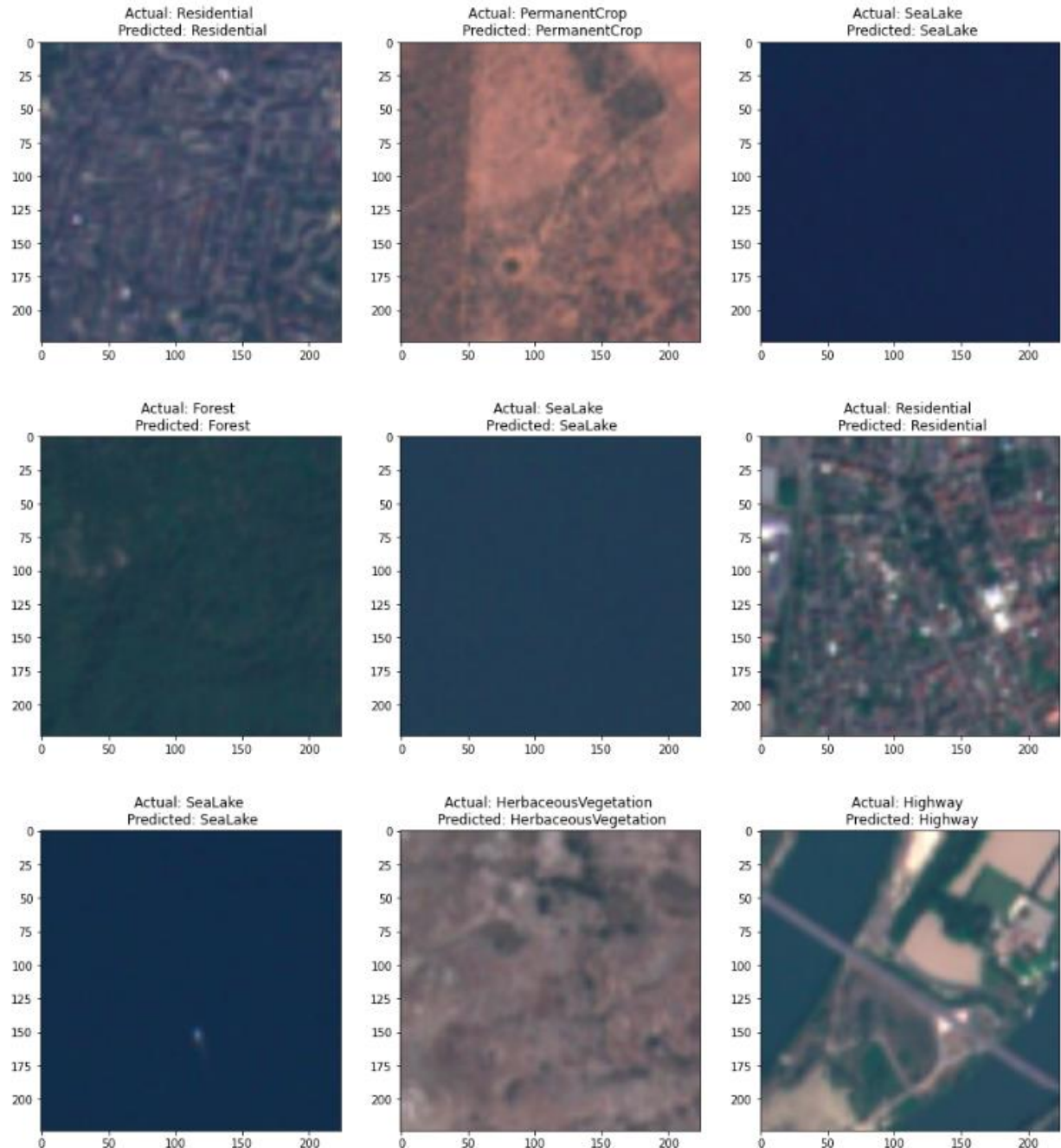


Fig. 10. Wide Resnet-50 Sample Results. It shows the actual and predicted values of sample inputs from test dataset.

6. Discussion

We have addressed the challenge of LULC classification using deep transfer learning techniques.

For this task, two prominent transfer learning architectures - VGG16 and Wide Resnet-50, with

the EuroSAT dataset have been used. Focusing on the LULC classification of the RGB bands of the EuroSAT dataset, we have achieved state-of-the-art accuracy of 99.17% by using the Wide Residual network (Wide Resnet-50).

Model	Epochs Trained	Total Time	Time per Epoch	Accuracy
VGG16 (Without Data Augmentation)	18	1h 47min 24s	5.9 min	98.14%
VGG16 (With Data Augmentation)	21	2h 4min 12s	6.1 min	98.55%
Wide Resnet 50 (Without Data Augmentation)	14	1h 19min 48s	5.5 min	99.04%
Wide Resnet 50 (With Data Augmentation)	23	2h 7min 53s	5.6 min	99.17%

Table 2: Comparative experimental results of VGG16 and WideResnet50 with and without data augmentation.

Experimentally we figured out the best fine-tuning parameters for VGG16 and Wide Resnet-50 with RGB bands of the EuroSAT dataset. The parameters that contributed to the best performance are used to create the final models. The models were compared with and without data augmentation. Both these architectures have been compared based on their computational training time, the number of epochs trained and test data accuracy (Table 2). From the results, it was observed that Wide Resnet-50 architecture is computationally more feasible as the time taken for each epoch to train is less than VGG16, even though the former is a deeper network.

The number of epochs trained is less without data augmentation, because of early stopping, since the data is limited. The model will converge early, not have much improvement, hence consuming

a shorter training time. In contrast, more epochs were trained with data augmentation because it generated more data for the model to learn the features from, which provided better generalisation and ultimately led to better accuracy.

Confusion matrices of the architectures have been provided (Fig. 6 &. 9). For Wide Resnet-50, we can see that the Forest class, followed by Sea Lake, was the best as it was hardly misclassified. Similarly, because of similar topological features herbaceous vegetation, annual crop, pasture and permanent crop were being confused. The Highway class was misclassified as river class because of a similar linear appearance. A similar trend was observed in the VGG16 confusion matrix. The presence of clear and distinct topological features for Forest and Sea Lake classes i.e. majority of green and blue cover for both the images led to accurate results. Similarly, pasture, herbaceous vegetation, annual crops were misclassified to higher degrees. Again, highway and river classification was also confused because of similar topological features. Thus, from these trends, we can conclude that model training was mimicking human learning patterns. With the presence of more inter and intra class variability in the dataset, these faulty learning patterns could be significantly improved. From the feature understanding capability depicted by the confusion matrices of both the models, we can see that the learning pattern of the architectures is quite comparable. The major difference lies only in how well the model is understanding everything i.e the classification accuracy.

We can see that the Wide Residual Network performed better than VGG16, both with and without data augmentation with accuracies of 99.04% and 99.17% respectively. Table 1 records the previous approaches for LULC classification with different models and bands from the EuroSAT

dataset. A notable accuracy of 98.74% was achieved by Li et al. with the DDRL-AM model [32]. However, the transfer learning approach - Wide Resnet-50 utilised in this paper gave a state-of-the-art accuracy of 99.17% with the RGB bands of the EuroSAT dataset.

7. Conclusion

Our objective with this paper was to investigate the use of transfer learning architectures for land use land cover classification. The study was based on two potential architectures - VGG16 and Wide Resnet-50, fine-tuned with RGB bands of the EuroSAT dataset for the classification. Much like the findings in other experiments, it was found that the transfer learning approach is quite reliable and produces the best overall results. The proposed methodology improves the state-of-the-art and provides a benchmark with an accuracy of 99.17% for the RGB bands of the EuroSAT dataset.

The classification results prior to and after data augmentation were compared. Data augmentation techniques elevate the diversification of the dataset as it only increases the visual variability of each training image without generating any new spectral or topological information. Evidently, the experimental results with data augmentation outperform those from the same model architecture trained on the original dataset. Model enhancement techniques like regularisation, early stopping, gradient clipping, learning rate optimisation etc. were implemented to make the model training more efficient, improve the performance and ultimately reduce the computational time required. Wide Resnet-50 architecture was found to generate better results than VGG16 while the same data augmentation approaches were applied for both. Even Though Wide Resnet-50 produced better results, the learning pattern of the models resembled, where the only difference was found in the accuracy of the class predictability.

This problem can be tackled by supplementing the quality and quantity of data. The generation of datasets with higher inter and intra class variability, backed by robust deep learning architectures with data augmentation techniques could effectively increase the representational power of the deep learning network. Thus the proposed methodology is effective exploitation of the satellite datasets available and deep learning approaches to achieve the best performance. The applications can be extended to multiple real-world earth observation applications for remote sensing scene analysis.

Supplementary Materials: Data associated with this research are available online. The EuroSAT dataset. The dataset is available for download at <https://github.com/phelber/eurosat>. The Jupyter Notebooks used for the training the image classifier is available for download at https://github.com/raoofnaushad/EuroSAT_LULC.

Author Contributions: Both the authors participated in preprocessing the datasets, creating the DL model architecture, training the model and evaluating the results. All authors have read and agreed to the published version of the manuscript.

Conflicts of Interest: The authors declare no conflict of interest.

References

1. Emery, W.; Camps, A. Chapter 1—The History of Satellite Remote Sensing. In *Introduction to Satellite Remote Sensing*; Emery, W., Camps, A., Eds.; Elsevier: Amsterdam, The Netherlands, 2017; pp. 1–42.

2. Zhou, Weixun & Newsam, Shawn & Li, Congmin & Shao, Zhenfeng. (2018). PatternNet: A benchmark dataset for performance evaluation of remote sensing image retrieval. *ISPRS Journal of Photogrammetry and Remote Sensing*. 145. 197-209. 10.1016/j.isprsjprs.2018.01.004.
3. Huang, Lanqing & Liu, Bin & Li, Boying & Guo, Weiwei & Yu, Wenhao & Zhang, Zenghui & Yu, Wenxian. (2017). OpenSARShip: A Dataset Dedicated to Sentinel-1 Ship Interpretation. *IEEE Journal of Selected Topics in Applied Earth Observations and Remote Sensing*. PP. 1-14. 10.1109/JSTARS.2017.2755672.
4. Basu, Saikat & ganguly, sangram & Mukhopadhyay, Supratik & Dibiano, Robert & Karki, Manohar & Nemani, Ramakrishna. (2015). DeepSat: a learning framework for satellite imagery. 1-10. 10.1145/2820783.2820816.
5. Yang, Yi & Newsam, Shawn. (2010). Bag-of-visual-words and spatial extensions for land-use classification. 270-279. 10.1145/1869790.1869829.
6. Qi, Kunlun & Wu, Huayi & Shen, Chen & Gong, Jianya. (2015). Land-Use Scene Classification in High-Resolution Remote Sensing Images Using Improved Correlatons. *IEEE Geoscience and Remote Sensing Letters*. 12. 1-5. 10.1109/LGRS.2015.2478966.
7. Pesaresi, Martino & Gerhardinger, A.. (2011). Improved Textural Built-Up Presence Index for Automatic Recognition of Human Settlements in Arid Regions With Scattered Vegetation. *Selected Topics in Applied Earth Observations and Remote Sensing, IEEE Journal of*. 4. 16 - 26. 10.1109/JSTARS.2010.2049478.
8. Buddhiraju, Krishna Mohan. (2011). Object-Based Image Analysis of High-Resolution Satellite Images Using Modified Cloud Basis Function Neural Network and Probabilistic

Relaxation Labeling Process. *IEEE T. Geoscience and Remote Sensing*. 49. 4815-4820. 10.1109/TGRS.2011.2171695.

9. Gaetano, Raffaele & Masi, Giuseppe & Poggi, Giovanni & Verdoliva, Luisa & Scarpa, Giuseppe. (2015). Marker-Controlled Watershed-Based Segmentation of Multiresolution Remote Sensing Images. *IEEE Transactions on Geoscience and Remote Sensing*. 53. 10.1109/TGRS.2014.2367129. Hu, F.; Xia, G.S.; Hu, J.; Zhang, L. Transferring deep convolutional neural networks of the scene classification of high-resolution remote sensing imagery. *Remote. Sens.* 2015, 7, 14680–14707.

10. Q. Zou, L. Ni, T. Zhang and Q. Wang, "Deep Learning Based Feature Selection for Remote Sensing Scene Classification," in *IEEE Geoscience and Remote Sensing Letters*, vol. 12, no. 11, pp. 2321-2325, Nov. 2015, doi: 10.1109/LGRS.2015.2475299.

11. Yin, Xiangnan & Chen, Weihai & Wu, Xingming & Yue, Haosong. (2017). Fine-tuning and visualization of convolutional neural networks. 1310-1315. 10.1109/ICIEA.2017.8283041.

12. Yosinski, J.; Clune, J.; Bengio, Y.; Lipson, H. How transferable are features in deep neural networks? In *Proceedings of the 27th International Conference on Neural Information Processing Systems*, Montreal, QC, Canada, 8–13 December 2014; Volume 27, pp. 3320–3328

13. Caruana, R. Learning Many Related Tasks at the Same Time with Backpropagation. In *Advances in Neural Information Processing Systems* 7; Tesauro, G., Touretzky, D.S., Leen, T.K., Eds.; MIT Press: Cambridge, MA, USA, 1995; pp. 657–664.

14. Bengio, Y. Deep Learning of Representations for Unsupervised and Transfer Learning. In Proceedings of the ICML Workshop on Unsupervised and Transfer Learning, Scotland, UK, 26 June–1 July 2012; Volume 27, pp. 17–36.
15. Xu, Jian & Song, Li & Zhong, De & Zhao, Zhi & Zhao, Kai. (2013). Remote Sensing Image Classification Based on a Modified Self-organizing Neural Network with a Priori Knowledge. *Sensors and Transducers*. 153. 29-36.
16. Chen, Yushi & Lin, Zhouhan & Zhao, Xing & Wang, Gang & Gu, Yanfeng. (2014). Deep Learning-Based Classification of Hyperspectral Data. *Selected Topics in Applied Earth Observations and Remote Sensing, IEEE Journal of*. 7. 2094-2107.
10.1109/JSTARS.2014.2329330.
17. Piramanayagam, S. & Schwartzkopf, W. & Koehler, Frederick & Saber, E.. (2016). Classification of remote sensed images using random forests and deep learning framework. 100040L. 10.1117/12.2243169.
18. Classification of remote sensed images using random forests and deep learning framework S. Piramanayagam, W. Schwartzkopf, F. W. Koehler, E. Saber. October 2016.
10.1117/12.2243169
19. Liu, Peng & Zhang, Hui & Eom, Kie. (2016). Active Deep Learning for Classification of Hyperspectral Images. *IEEE Journal of Selected Topics in Applied Earth Observations and Remote Sensing*. PP. 1-13. 10.1109/JSTARS.2016.2598859.
20. Yu, Xingrui & Wu, Xiaomin & Luo, Chunbo & Ren, Peng. (2017). Deep learning in remote sensing scene classification: a data augmentation enhanced convolutional neural network framework. *GIScience & Remote Sensing*. 54. 1-18.
10.1080/15481603.2017.1323377.

21. Yang, Zhou & Mu, Xiao-dong & Zhao, Feng-an. (2018). Scene classification of remote sensing image based on deep network and multi-scale features fusion. *Optik*. 171. 10.1016/j.ijleo.2018.06.024.

22. D. Guo, Y. Xia and X. Luo, "Scene Classification of Remote Sensing Images Based on Saliency Dual Attention Residual Network," in *IEEE Access*, vol. 8, pp. 6344-6357, 2020, doi: 10.1109/ACCESS.2019.2963769.

23. Xu, Xiaowei & Chen, Yinrong & Zhang, Junfeng & Chen, Yu & Anandhan, Prathik & Manickam, Adhiyaman. (2020). A novel approach for scene classification from remote sensing images using deep learning methods. *European Journal of Remote Sensing*. 54. 1-13. 10.1080/22797254.2020.1790995.

24. Alhichri, Haikel & Alsuwayed, Asma & Bazi, Yakoub & Ammour, Nassim & Alajlan, Naif. (2021). Classification of Remote Sensing Images Using EfficientNet-B3 CNN Model With Attention. *IEEE Access*. PP. 1-1. 10.1109/ACCESS.2021.3051085.

25. Castelluccio, Marco & Poggi, Giovanni & Sansone, Carlo & Verdoliva, Luisa. (2015). Land Use Classification in Remote Sensing Images by Convolutional Neural Networks. Aug 2015, arXiv:1508.00092.

26. Y. Liang, S. T. Monteiro and E. S. Saber, "Transfer learning for high resolution aerial image classification," 2016 IEEE Applied Imagery Pattern Recognition Workshop (AIPR), 2016, pp. 1-8, doi: 10.1109/AIPR.2016.8010600.

27. Pires de Lima, Rafael & Marfurt, (2019). Convolutional Neural Network for Remote-Sensing Scene Classification: Transfer Learning Analysis. *Remote Sensing*. 12. 86. 10.3390/rs12010086.

28. A. Bahri, S. Ghofrani Majelan, S. Mohammadi, M. Noori and K. Mohammadi, "Remote Sensing Image Classification via Improved Cross-Entropy Loss and Transfer Learning Strategy Based on Deep Convolutional Neural Networks," in IEEE Geoscience and Remote Sensing Letters, vol. 17, no. 6, pp. 1087-1091, June 2020, doi: 10.1109/LGRS.2019.2937872.

29. Helber, Patrick & Bischke, Benjamin & Dengel, Andreas & Borth, Damian. (2017). EuroSAT: A Novel Dataset and Deep Learning Benchmark for Land Use and Land Cover Classification. 10.1109/JSTARS.2019.2918242.

30. G. Chen, X. Zhang, X. Tan, Y. Cheng, F. Dai, K. Zhu, Y. Gong, Q. Wang. Training Small Networks for Scene Classification of Remote Sensing Images via Knowledge Distillation. *Remote Sens.* 2018, 10, 719. doi:10.3390/rs10050719, 2018.

31. N. Sonune. Land Cover Classification with EuroSAT Dataset.
<https://www.kaggle.com/nilesh789/land-cover-classification-with-eurosat-dataset>, 2020.

32. Li, Jun & Lin, Daoyu & Wang, Yang & Xu, Guangluan & Zhang, Yunyan & Ding, Chibiao & Zhou, Yanhai. (2020). Deep Discriminative Representation Learning with Attention Map for Scene Classification. *Remote Sensing*. 12. 1366. 10.3390/rs12091366.

33. Hadi Yassine, K. Tout, Mohamed Jaber Improving LULC Classification from Satellite Imagery using Deep Learning - Eurosat Dataset K. Tout; Hadi Yassine Hamdi; Yassine Mohamad; Jaber Mohamad Jaber, 10.5194/isprs-archives-XLIII-B3-2021-369-2021

34. Simonyan, Karen & Zisserman, Andrew. (2014). Very Deep Convolutional Networks for Large-Scale Image Recognition. *arXiv* 1409.1556.

35. H. Jung, M. Choi, J. Jung, J. Lee, S. Kwon and W. Y. Jung, "ResNet-Based Vehicle Classification and Localization in Traffic Surveillance Systems," 2017 IEEE Conference

on Computer Vision and Pattern Recognition Workshops (CVPRW), 2017, pp. 934-940, doi: 10.1109/CVPRW.2017.129.

36. Devvi Sarwinda, Radifa Hilya Paradisa, Alhadi Bustamam, Pinkie Anggia, Deep Learning in Image Classification using Residual Network (ResNet) Variants for Detection of Colorectal Cancer, Procedia Computer Science, Volume 179, 2021, Pages 423-431, ISSN 1877-0509, <https://doi.org/10.1016/j.procs.2021.01.025>.

37. A. S. B. Reddy and D. S. Juliet, "Transfer Learning with ResNet-50 for Malaria Cell-Image Classification," 2019 International Conference on Communication and Signal Processing (ICCSP), 2019, pp. 0945-0949, doi: 10.1109/ICCSP.2019.8697909.

38. Monti, Ricardo & Tootoonian, Sina & Cao, Robin. (2018). Avoiding Degradation in Deep Feed-Forward Networks by Phasing Out Skip-Connections: 27th International Conference on Artificial Neural Networks, Rhodes, Greece, October 4–7, 2018, Proceedings, Part III. 10.1007/978-3-030-01424-7_44.

39. K. He, X. Zhang, S. Ren and J. Sun, "Deep Residual Learning for Image Recognition," 2016 IEEE Conference on Computer Vision and Pattern Recognition (CVPR), 2016, pp. 770-778, doi: 10.1109/CVPR.2016.90.

40. Zagoruyko, Sergey & Komodakis, Nikos. (2016). Wide Residual Networks. May 2016, arXiv:1605.07146

41. Mikołajczyk, Agnieszka & Grochowski, Michał. (2018). Data augmentation for improving deep learning in image classification problem. 117-122. 10.1109/IIPHDW.2018.8388338.

42. The Effectiveness of Data Augmentation in Image Classification using Deep Learning. Luis Perez, Jason Wang, Dec 2017, arXiv:1712.04621

43. Why gradient clipping accelerates training: A theoretical justification for adaptivity.
Jingzhao Zhang, Tianxing He, Suvrit Sra, Ali Jadbabaie, May 2019, arXiv:1905.11881
44. Xiao-Hu Yu, Guo-An Chen and Shi-Xin Cheng, "Dynamic learning rate optimization of the backpropagation algorithm," in IEEE Transactions on Neural Networks, vol. 6, no. 3, pp. 669-677, May 1995, doi: 10.1109/72.377972.
45. J. Konar, P. Khandelwal and R. Tripathi, "Comparison of Various Learning Rate Scheduling Techniques on Convolutional Neural Network," 2020 IEEE International Students' Conference on Electrical, Electronics and Computer Science (SCEECS), 2020, pp. 1-5, doi: 10.1109/SCEECS48394.2020.94.